

Preparation of mitochondria to measure superoxide flashes in angiosperm flowers

Chulan Zhang^{Equal first author, 1}, Fengshuo Sun^{Equal first author, 2}, Biao Xiong³, Zhixiang Zhang^{Corresp. 1}

¹ College of Nature Conservation, Beijing Forestry University, Beijing, China

² College of Biological Sciences and Biotechnology, Beijing Forestry University, Beijing, China

³ College of Tea Science, Guizhou University, Guizhou Province, China

Corresponding Author: Zhixiang Zhang

Email address: zxzhang@bjfu.edu.cn

Background Mitochondria are the center of energy metabolism and the production of reactive oxygen species (ROS). ROS production results in a burst of “superoxide flashes”, which is always accompanied by depolarization of mitochondrial membrane potential. Superoxide flashes have only been studied in the model plant *Arabidopsis thaliana* using a complex method to isolate mitochondria. In this study, we present an efficient, easier method to isolate functional mitochondria from floral tissues to measure superoxide flashes.

Method We used 0.5 g samples to isolate mitochondria within < 1.5 h from flowers of two non-transgenic plants (*Magnolia denudata* and *Nelumbo nucifera*) to measure superoxide flashes. Superoxide flashes were visualized by the pH-insensitive indicator MitoSOX Red, while the mitochondrial membrane potential ($\Delta\Psi_m$) was labelled with TMRM.

Results Mitochondria isolated using our method showed a high respiration ratio. Our results indicate that the location of ROS and mitochondria was in a good coincidence. Increased ROS together with a higher frequency of superoxide flashes was found in mitochondria isolated from the flower pistil. Furthermore, a higher rate of depolarization of the $\Delta\Psi_m$ was observed in the pistil. Taken together, these results demonstrate that the frequency of superoxide flashes is closely related to depolarization of the $\Delta\Psi_m$ in petals and pistils of flowers.

1 **Preparation of mitochondria to measure superoxide**
2 **flashes in angiosperm flowers**

3

4 Chulan Zhang¹, Fengshuo Sun², Biao Xiong³, and Zhixiang Zhang¹

5 ¹ College of Nature Conservation, Beijing Forestry University, Beijing, China

6 ² College of Biological Sciences and Biotechnology, Beijing Forestry University, Beijing, China

7 ³ College of Tea Science, GuiZhou University, GuiZhou Province, China

8

9 **Corresponding author:**

10 Zhixiang Zhang, Ph.D.

11 Qinghua East Street, Beijing, 100083, China

12 E-mail: zxzhang@bjfu.edu.cn

13

14

15

16

17

18

19

20

21

22

23

24 **Abstract**

25 **Background** Mitochondria are the center of energy metabolism and the production of reactive
26 oxygen species (ROS). ROS production results in a burst of “superoxide flashes”, which is
27 always accompanied by depolarization of mitochondrial membrane potential. Superoxide flashes
28 have only been studied in the model plant *Arabidopsis thaliana* using a complex method to
29 isolate mitochondria. In this study, we present an efficient, easier method to isolate functional
30 mitochondria from floral tissues to measure superoxide flashes.

31 **Method** We used 0.5 g samples to isolate mitochondria within < 1.5 h from flowers of two non-
32 transgenic plants (*Magnolia denudata* and *Nelumbo nucifera*) to measure superoxide flashes.
33 Superoxide flashes were visualized by the pH-insensitive indicator MitoSOX Red, while the
34 mitochondrial membrane potential ($\Delta\Psi_m$) was labelled with TMRM.

35 **Results** Mitochondria isolated using our method showed a high respiration ratio. Our results
36 indicate that the location of ROS and mitochondria was in a good coincidence. Increased ROS
37 together with a higher frequency of superoxide flashes was found in mitochondria isolated from
38 the flower pistil. Furthermore, a higher rate of depolarization of the $\Delta\Psi_m$ was observed in the
39 pistil. Taken together, these results demonstrate that the frequency of superoxide flashes is
40 closely related to depolarization of the $\Delta\Psi_m$ in petals and pistils of flowers.

41

42

43

44

45

46

47

48

49

50

51 **Introduction**

52 Mitochondria are widely distributed organelles in eukaryotic cells where they perform
53 important roles generating energy, regulating physiological activities, and maintaining cellular
54 metabolism (Hatefi 1985; Yang et al. 2018). The major role of mitochondria is the generation of
55 ATP by oxidative phosphorylation through the electron transport chain (Hatefi 1985). In addition
56 to energy production, mitochondria are also the center of reactive oxygen species (ROS)
57 production in organisms under biotic or abiotic stress (Paital and Chainy 2014; Yang et al. 2016).
58 The isolation of mitochondria has deepened research on metabolism and stress in plants (Day et
59 al. 1985). In 1985, mitochondria from 300 g of pea leaves were isolated and purified by
60 centrifugation on a Percoll gradient containing a linear gradient of polyvinylpyrrolidone-25 (0–
61 10%, w/v) to obtain only 20 mg mitochondrial protein (Day et al. 1985). After that, mitochondria
62 were isolated from *Arabidopsis thaliana* using differential centrifugation and further purified
63 using a continuous colloidal density gradient (Lyu et al. 2018; Sweetlove et al. 2007). In
64 addition, crude isolation of mitochondria in leaves using density gradient centrifugation revealed
65 higher respiratory coupling than that observed in purified mitochondria (Keech et al. 2005). It is
66 well known that mitochondria must be purified to extract mitochondrial DNA and the proteome
67 (Ahmed and Fu 2015; Kim et al. 2015), but the time required and the sampling method were not
68 suitable in many mitochondrial studies, particularly in non-green tissues such as flowers. Crude
69 isolation of the intact and functional mitochondria is crucial for the measurement of superoxide
70 flashes in plants.

71

72 Superoxide flashes are 10-s events that occur spontaneously and suddenly in mitochondria
73 and reflect electrical and chemical activities (Feng et al. 2017). Superoxide flashes were first
74 defined as transient events of the mitochondrial matrix-targeted biosensor mt-cp YFP (Wei and

75 Dirksen 2012). As mt-cp YFP is sensitive to pH, superoxide flashes can be visualized by
76 chemical probes, including ROS indicators, such as MitoSOX for superoxide and 2,7-
77 dichlorodihydrofluorescein (DCF) for H₂O₂ (Feng et al. 2017; Zhang et al. 2013). Interestingly,
78 cp-YFP superoxide flashes are correlated with depolarization of
79 the mitochondrial membrane potential ($\Delta\Psi_m$) (Zhang et al. 2013). Previous studies have shown
80 that ROS modulate a variety of physiological events, including growth, stress, thermogenesis,
81 and diseases (Jastroch 2017; Keunen et al. 2015; Kuznetsov et al. 2017; Maksimov et al. 2018;
82 Yang et al. 2016). It is clear that the accumulation of ROS are closely associated with superoxide
83 flashes. In animals, superoxide flashes and ROS bursts are involved in various physiological
84 activities, such as oxidative stress, metabolism, and aging (Pouvreau 2010; Wei et al. 2011).
85 Thus, there is a close relationship between superoxide flashes and mitochondrial energy
86 metabolism. Considering the importance of the mitochondrial respiratory chain and energy
87 metabolism, it is of great significance to study mitochondrial superoxide flashes in plants.

88

89 Superoxide flashes have been well studied in cells and isolated mitochondria of animals, and
90 the cp YFP-flash signals are always associated with the loss of $\Delta\Psi_m$ (labeled with TMRM) (Li et
91 al. 2012). Superoxide flashes observed with the chemical probes MitoSOX and DCF reveal the
92 same results and frequency as cp YFP flashes (Zhang et al. 2013). In plant tissues, superoxide
93 flashes have only been studied in the roots of Arabidopsis and the cp-YFP signals changed with
94 different respiratory substrates (Schwarzlander et al. 2011), but no study has explored superoxide
95 flashes in other non-transgenic tissues of plants. Floral tissues in plants are important organs
96 involved in various physical activities, including thermogenesis, pollination, and reproduction
97 (Luo et al. 2010; Thien et al. 2009). Mitochondrial energy metabolism and oxygen consumption
98 are closely related to floral thermogenesis and reproduction (Miller et al. 2011); thus, it is
99 necessary to combine the activity of mitochondrial superoxide flashes with a study of floral
100 reproduction in plants. As isolating plant mitochondria using a previous method was likely to
101 influence mitochondrial viability and the mitochondrial-targeted cp-YFP is hardly expressed in

102 xylophyta flowers, a suitable method to study superoxide flashes in floral tissues is crucial.

103 To address these issues, some important modifications were devised based on previous
104 methods to study superoxide flashes (Zhang et al. 2013). We developed an efficient method to
105 isolate high viability mitochondria in floral tissues of *Magnolia denudata* and *Nelumbo nucifera*.
106 As these are non-transgenic flowers, superoxide flashes were first visualized by loading the
107 plants with MitoSOX Red, while the $\Delta\Psi_m$ was labelled with TMRM. These methods facilitated
108 study of mitochondrial energy metabolism and physiological activities in non-transgenic flowers
109 of angiosperms. This quick and sample-saving protocol greatly improved the viability of
110 mitochondria and efficiency of the experiment of superoxide flashes in non-green plant tissues.

111

112

113 **Materials & Methods**

114 **Plant materials/plant growth**

115 *M. denudata* was grown on the campus of Beijing Forestry University (40°00'02"N,
116 116°20'15", a.s.l., 60 m). Pistils and petals of 15 flowers were collected during afternoons in
117 March and April. *N. nucifera* was grown in Bajia Country Park (40°00'50"N, 116°19'39"E, a.s.l.,
118 47 m). Receptacles and petals of nearly 10 flowers were collected during afternoons in July–
119 August.

120

121 **Solutions**

122 Method A: Grinding buffer: 0.3 M sucrose, 25 mM Na₄P₂O₄, 2 mM EDTA, 10 mM
123 KH₂PO₄, 1% (w/v) polyvinylpyrrolidone-40, 1% (w/v) defatted bovine serum albumin (BSA), 4
124 mM cysteine, and 20 mM ascorbic acid were added just prior to grinding. pH was adjusted to 7.5
125 with KOH. Resuspension buffer: 0.3 M sucrose, 10 mM N-Tris [hydroxymethyl]-methyl-2-
126 aminoethanesulfonic acid (TES-KOH), and 0.1% BSA, pH = 7.5. Mitochondrial basic incubation
127 medium: 0.3 M sucrose, 10 mM TES-KOH. 10 mM NaCl, 5 mM KH₂PO₄, 2 mM MgSO₄, and
128 0.1% BSA, pH = 7.2.

129 Method B: Grinding buffer: 0.3 M sucrose, 25 mM Na₄P₂O₄, 2 mM EDTA, 10 mM
130 KH₂PO₄, 1% (w/v) polyvinylpyrrolidone-40, 1% (w/v) defatted bovine serum albumin (BSA)
131 and 20 mM ascorbic acid were added just prior to grinding. pH was adjusted to 7.5 with KOH.
132 Resuspension buffer: 0.3 M sucrose and 10mM TES-KOH, pH = 7.5. Preparation of a single
133 linear PVP-40 gradient in 28% (v/v) Percoll: 0.3 M sucros, 10 mM KH₂PO₄, 0.1% BSA, 28%
134 (v/v) Percoll and a linear gradient of 0-10% (w/v) PVP-40 (top to bottom) in a 30 ml centrifuge
135 tube. pH = 7.2. Mitochondrial basic incubation medium: 0.3 M sucrose, 10 mM TES-KOH. 10
136 mM NaCl, 5 mM KH₂PO₄, 2 mM MgSO₄, and 0.1% BSA, pH = 7.2.

137

138 **Isolation of mitochondria**

139 Method A: Our efficiency method to obtain crude, high viability mitochondria. All steps
140 were carried at 4°C on ice. Mitochondria of magnolia were isolated from style and petal tissues
141 while mitochondria of lotus were isolated from receptacle and petal tissues. About 0.5 g of pistil
142 or petal tissues were cut up from each species into 1 mm³-fragments with scissors. They were
143 ground in 1–2 ml of grinding buffer using a pestle with a small amount of quartz. The extract
144 was filtered through 20 µm nylon mesh and then centrifuged at 2,000 × g for 10 min to remove
145 most of the thylakoid membranes and intact chloroplasts. The supernatant was transferred to a
146 new tube and centrifuged at 12,000 × g for 20 min. The pellet was resuspended in 1 ml
147 resuspension buffer and centrifuged for 5 min at 1,500 × g to remove the residual intact
148 chloroplasts. This new supernatant was centrifuged for 20 min at 12,000 × g to yield the crude
149 mitochondria. The crude mitochondria were suspended in mitochondrial basic incubation
150 medium and placed on ice for further studies.

151 Method B: to obtain purified mitochondria as previous study. All steps were carried at 4°C
152 on ice. Mitochondria were isolated from style of magnolia and receptacle of lotus. About 45 g of
153 pistil tissues were cut up with scissors (see above). Isolation of mitochondria was based on the
154 method of Sweetlove *et al* (2007) with minor modification. Briefly, pistil tissues were blended in
155 200 ml grinding buffer (see above), filtered through 20 µm nylon mesh and then centrifuged at

156 1,100 × g for 10 min. The supernatant was centrifuged at 18,000 × g for 20 min. The pellet was
157 resuspended in 30 ml resuspension buffer and centrifuged for 10 min at 1,100 × g. This new
158 supernatant was centrifuged for another 20 min at 18,000 × g. The final pellet was suspended in
159 1 ml resuspension buffer and layered over the linear PVP-40 gradient in 28% (v/v) Percoll (see
160 above), and centrifuged for 45 min at 40,000 × g. The mitochondria were found in a tight white
161 band near the bottom of tube. The mitochondria fraction was carefully removed and resuspended
162 in 20 ml resuspension buffer, the suspension was centrifuged for 20 min at 15,000 × g. The
163 purified mitochondria were suspended in mitochondrial basic incubation medium and place on
164 ice for further studies.

165

166 **Mitochondrial respiratory function assay**

167 The oxygen consumption rates of mitochondria were determined with a Clark-type oxygen
168 electrode (Strathkelvin 782 2-Channel Oxygen System version 1.0, Strathkelvin Instruments,
169 Motherwell, UK) at 25°C. A 10 µl aliquot of mitochondrial suspension was blended in 1 ml of
170 mitochondrial basic incubation medium. The oxygen sensor signal was recorded on a computer
171 at intervals of 0.5 s with Strathkelvin Instruments software (782 System version 1.0). Oxygen
172 consumption was measured with 250 µM ADP (state 3) and with 5 mM succinate (state 4). The
173 respiratory control ratio (RCR) was calculated as the ratio of state 3 to state 4 respiration. The
174 mitochondrial suspensions with higher than a state 3 RCR were used in subsequent studies.

175

176 **Confocal imaging of Mito-ROS and $\Delta\Psi_m$**

177 To visualize the superoxide flashes and $\Delta\Psi_m$, isolated mitochondria from pistil and petal
178 tissues of magnolia and lotus were immobilized on round glass cover slides (pretreatment with
179 0.2 mg/ml poly-L-lysine for 1 h; Sigma, St. Louis, MO, USA) by centrifugation at 2,000 × g for
180 5 min at 4°C and mounted on an inverted microscope (Zeiss LSM 710: Carl Zeiss, Oberkochen,
181 Germany) for imaging. To measure the subcellular locations of mitochondria and ROS,
182 mitochondria were first incubated with 100 nM MitoTracker Green (Invitrogen, Carlsbad, CA,
183 USA) for 30 min at 25°C and washed in mitochondrial basic incubation medium, then loaded

184 with 2.5 μM MitoSOX Red for 5 min. MitoTracker Green was excited with 488 nm and
185 emissions were collected at 500–530 nm, while MitoSOX Red was excited with 543 nm and
186 collected at an emission wavelength of 560–620 nm. Isolated mitochondria were labelled with
187 2.5 μM MitoSOX Red and 5 mM succinate as a respiration substrate to measure superoxide
188 flashes. To understand the MitoSOX-flashes behavior in the change of respiration state and
189 uncoupler, 0.25 mM ADP and 5 μM FCCP (Carbonyl cyanide 4-(trifluoromethoxy)
190 phenylhydrazone) was added to observe the superoxide flashes. Isolated mitochondria were
191 loaded with 50 nM TMRM and 5 mM succinate for 1 min at 25°C to measure the $\Delta\Psi_m$. The
192 excitation wavelength for TMRM was 543 and the emission wavelength was 550–620 nm. A
193 total of 100 frames of 512×512 pixels were collected for a typical time-series recording. The
194 frame rate was 50–60 frames/min. All experiments were performed at room temperature (24–
195 26°C).

196

197 **Data analysis**

198 The images obtained by laser scanning confocal microscopy were analyzed using Image J
199 1.48v (Wayne Rasband, National Institutes of Health, Bethesda, MD, USA). Superoxide flashes
200 and variations in the $\Delta\Psi_m$ were identified using FlashSniper (Li et al. 2012), and their
201 morphological, properties, and duration were measured automatically. Statistical analyses were
202 performed using SPSS Statistics 23.0 software (IBM Corp., Armonk, NY, USA). Images were
203 processed and assembled using Adobe Photoshop CS 5 (Adobe Systems Corp., San Jose, CA,
204 USA).

205

206

207

208 **Results**

209 **Respiratory function and viability of isolated mitochondria**

210 Crude mitochondria were sampled from petal and style tissues of magnolia as shown in Fig.

211 1A, while mitochondria from petal and receptacle tissues of lotus were sampled as shown in Fig.
212 1F. A signal with excitation at 488 nm was confirmed to avoid the disturbing auto-fluorescence
213 of intact chloroplasts. As shown in Fig. 1B and G, no intact chloroplasts were detected in the
214 crude isolated mitochondria. To compare the previous method (method B) (Day et al. 1985) and
215 our efficient method (method A) to isolate mitochondria, the respiratory function of the isolated
216 mitochondria was determined with a Clark-type oxygen electrode. As a result, the RCR did not
217 change significantly in mitochondria isolated from flowers using method A ($n = 6$), but RCR
218 declined in isolated mitochondria using method B ($n = 6$) (Table 1). As the viability of
219 mitochondria is reflected by the $\Delta\Psi_m$, crude isolated mitochondria were loaded with the TMRM
220 indicator. Highly viable and highly dense mitochondria were observed in mitochondria of
221 magnolia (Fig. 1C, D) and lotus (Fig. 1H, I). The viability of mitochondria using method B was
222 lower than that of method A (Fig. 1E, J). We assessed the time consumed, amount of sample
223 consumed, and the viability of both methods. Using method B, mitochondria were processed in
224 5.28 ± 0.23 h and consumed 43.92 ± 3.78 g of flower tissues ($n = 6$), whereas mitochondria were
225 isolated within 1.13 ± 0.14 h with only 0.47 ± 0.12 g tissues ($n = 6$) using our method A. This
226 result shows that our mitochondrial isolation method was highly efficient to obtain highly viable
227 mitochondria in the flower species.

228

229 **ROS production in floral mitochondria**

230 To identify the intracellular site of ROS production, mitochondrial ROS were loaded with
231 MitoSOX Red for 5 min ($2.5 \mu\text{M}$), while mitochondria were loaded with Mito Tracker Green for
232 30 min (100 nM). ROS production and mitochondrial location were coincident in the
233 mitochondria isolated from petals and styles of magnolia, suggesting that mitochondria are the
234 primary site of ROS production in this species (Fig. 2C, G). The same results were found in the
235 mitochondria isolated from receptacle and petal of lotus (Fig. 2J, N).

236 The fluorescent level of ROS increased significantly in the mitochondria isolated from style
237 compared to the petal of magnolia (Fig. 2B, D, F) ($n = 100$). In addition, similar results were

238 found in the isolated mitochondria of lotus, as the ROS level was significantly higher in the
239 receptacle than in the petal (Fig. 2I, K, M) ($n = 100$). Our results confirm that mitochondrial
240 ROS tended to accumulate in the pistil of both magnolia and lotus, indicating that mitochondrial
241 ROS might be more involved in the electron transport chain in the pistil than in the petal.

242

243 **Superoxide flashes in flowers**

244 To investigate the nature of superoxide flashes in magnolia and lotus, isolated mitochondria
245 were loaded with the ROS fluorescent probe MitoSOX Red with 5 mM succinate added as
246 respiratory substrate. According to a previous study (Wang et al. 2016b), we defined the
247 variation of fluorescence at $df/F_0 > 0.2$ within 10 s as a single superoxide flash event. A transient
248 increase in MitoSOX fluorescence and variations in the trace were observed during 100 s in
249 single mitochondrial events (Fig. 3A, B, and Video S1). Among these instantaneous traces, three
250 types of mitochondrial superoxide traces were classified (Fig. 3C, D, E): low variation slope
251 traces ($0.2 < df/F_0 < 0.5$) (Fig. 3C), high variation slope traces ($0.5 \leq df/F_0$) (Fig. 3D), and multi-
252 event traces ($0.2 < df/F_0$) (Fig. 3E). We also compared the frequency of superoxide flashes ($/100s$
253 $\times 1,000 \mu\text{m}^2$) in mitochondria isolated from petals and pistils of magnolia and lotus. Notably,
254 superoxide oxide flashes labelled with MitoSOX Red were detected at a rate of 129.18 ± 20.11
255 ($/100 \text{ s} \times 1,000 \mu\text{m}^2$, $n = 13$) in mitochondria isolated from the magnolia style (Fig. 3F) which
256 was significantly higher than mitochondria in the petal ($75.23 \pm 10.48/100 \text{ s} \times 1,000 \mu\text{m}^2$, $n =$
257 11). In lotus (Fig. 3G), the rate of superoxide flashes was 48.24 ± 10.24 ($/100 \text{ s} \times 1,000 \mu\text{m}^2$, $n =$
258 10) in mitochondria isolated from the style, which was also significantly higher than
259 mitochondria in the petal ($25.68 \pm 4.79 /100 \text{ s} \times 1,000 \mu\text{m}^2$, $n = 10$). These results indicate that
260 superoxide flashes, together with ROS bursts, are highly autonomous and predominantly reflect
261 the properties and physical activities of mitochondria in different tissues and species.

262 The MitoSOX-flashes were closely linked to functional ETC and respiratory activity. To
263 observe the mitochondrial behavior in the change of respiration state and uncoupler, 0.25 mM
264 ADP and 5 μM FCCP was added for the measurement of mitochondria isolated from style of

265 Magnolia. The addition of ADP resulted in a significantly decrease in MitoSOX fluorescence
266 (Fig B, D) (n=100). Mitochondrial respiratory uncoupled by FCCP also led to the significantly
267 decrease in MitoSOX signal (Fig 4C, D) (n=100). Similar behavior was found in the
268 measurement of MitoSOX-flashes, the rate of superoxide flashes with succinate was significantly
269 higher than mitochondria in the addition of ADP and FCCP (Fig 4E) (n=6). Low flashes
270 occurred in mitochondria upon uncoupling suggested that the electrical transmembrane gradient
271 might modulate the superoxide flashes.

272

273 **Depolarization of the mitochondrial membrane potential in flowers**

274 To study variations in the $\Delta\Psi_m$, isolated mitochondria were labelled with TMRM, and 5 mM
275 of succinate was added. The decline in fluorescent intensity at $df/F_0 < -0.2$ was defined as an
276 event. Transient depolarization of the $\Delta\Psi_m$ accompanied by later polarization occurred in a
277 single mitochondrion (Fig. 5A, B and Video S2). According to the wide variation in $\Delta\Psi_m$, the
278 trace $\Delta\Psi_m$ was catalogued into three types (Fig. 5C, D, E): Instantaneous loss of $\Delta\Psi_m$ along
279 with instant recovery (Fig. 5C), instantaneous loss of $\Delta\Psi_m$ with a short period of stability before
280 recovery (Fig. 5D), and multi-event trace including the above two types (Fig. 5E). The frequency
281 of a TMRM-event in mitochondria isolated from magnolia petals ($544.92 \pm 56.98 / 100 \text{ s} \times 1,000$
282 μm^2 , n = 15) was significantly lower than the values in the style ($1,009.10 \pm 130.10 / 100 \text{ s} \times$
283 $1,000 \mu\text{m}^2$, n = 15) (Fig. 5G). The same result was found in lotus (Fig. 5F) that the frequency of
284 TMRM events in mitochondria isolated from the lotus petal was $51.94 \pm 10.57 (/100 \text{ s} \times 1,000$
285 μm^2 , n = 10) which was lower than that in the receptacle ($119.99 \pm 19.00 / 100 \text{ s} \times 1,000 \mu\text{m}^2$, n =
286 10). We conclude that transient and spontaneous depolarization of $\Delta\Psi_m$ occurred in all tissues
287 and the higher frequency of variation of $\Delta\Psi_m$ in the pistils of flowers suggest that they have a
288 higher level of mitochondrial dynamics.

289

290

291 Discussion

292 Isolating mitochondria from plant tissues is complex and inefficient. In a previous study, the
293 sucrose-based differential centrifugation method requires high-speed centrifugation ($40,000 \times g$)
294 and 300 g of sample within 5 h to obtain purified mitochondria (Day et al. 1985). Isolating
295 mitochondria using the colloidal density gradient method consumes 60 g of sample and more
296 than 4 h (Sweetlove et al. 2007). These methods are time- and sample-consuming, which may
297 hinder the function and respiratory coupling of the mitochondria. In our method, we used only
298 0.5 g of floral tissues to obtain crude functional mitochondria in less than 1.5 h after
299 centrifugation at a low speed ($\leq 12,000 \times g$), which only required a standard laboratory
300 centrifuge. A previous study reported that isolating crude mitochondria from leaves results in a
301 higher RCR than when isolating purified mitochondria, which was consistent with our results
302 (Keech et al. 2005). Since high mitochondrial respiration control ratio was prerequisite for
303 superoxide flashes to occur (Schwarzlander et al. 2011), isolation of high viability mitochondria
304 was necessary for the measurement of superoxide flashes. In the present study, we provide an
305 effective and simple method to obtain highly viable mitochondria in different flower tissues to
306 measure mitochondrial ROS, superoxide flashes and the $\Delta\Psi_m$.

307 Mitochondrial ROS modulate various physiological events, including stress, growth, and cell
308 death (Dickinson and Chang 2011; NavaneethaKrishnan et al. 2018; Sundaresan et al. 1995).
309 Colocalization of ROS and mitochondria in polar growing pollen tubes reveals the production of
310 H_2O_2 in mitochondria during pollen germination (Maksimov et al. 2018). Also, ROS are
311 produced in mitochondria until the full flower bloom stage (Chakrabarty et al. 2007; Rogers
312 2012). Our study found good coincidence between the location of ROS and mitochondria in
313 petals and pistils of two flower species (Fig. 2), indicating that ROS originate in mitochondria
314 from floral tissues. ROS always act as signaling molecules to unlock the antioxidant system and
315 maintain physiological activities in plants under salt stress (Ahanger et al. 2017). ROS are also
316 involved in the energy-dissipating system that increases frost resistance in seedlings under
317 freezing conditions (Grabelnych et al. 2014). And mitochondria contribute to ROS production

318 through electron transfer from the respiratory chain in non-green tissues, such as flowers, and
319 ROS homeostasis is regulated by the antioxidant system (Rhoads et al. 2006; Rogers and Munne-
320 Bosch 2016). Considering the increased mitochondrial ROS production in pistils of magnolia
321 and lotus in our study, mitochondrial ROS might be more involved in the respiratory metabolic
322 signaling pathways in the pistils of these two flower species.

323 An increase in ROS accumulation can trigger ROS burst in plants (Zandalinas and Mittler
324 2018), and basal mitochondrial ROS production is intimately linked with ROS flashes (Wang et
325 al. 2012). The basal elevation of mitochondrial ROS triggers superoxide flashes (Hou et al.
326 2013). In our results, the simultaneous increase in ROS production and the frequency of
327 superoxide flashes in the pistils indicated that increasing ROS production might trigger
328 superoxide flashes. Superoxide flashes are involved in various stressful and pathophysiological
329 conditions (Fang et al. 2011; Wang et al. 2013). Superoxide flashes are sensitive to
330 mitochondrial respiration and a higher frequency of superoxide flash events acts as an early
331 mitochondrial signal in response to physiological activities and oxidative stress (Ma et al. 2011;
332 Wei et al. 2011). Superoxide flashes always respond to metabolic activities and act as a signal
333 mediating disease (Cao et al. 2013; Wang et al. 2013). In addition, the frequency of superoxide
334 flashes in early adulthood predicts the lifespan of an organism (Shen et al. 2014). Similarly,
335 changes in superoxide flashes and fluorescence are closely related to respiratory activity in
336 Arabidopsis and are affected by different respiratory substrates and inhibitors (Schwarzlander et
337 al. 2011). Considering that superoxide flashes visualized by MitoSOX occurred at a similar
338 frequency as cp-YFP-flashes in previous studies (Wang et al. 2016a; Zhang et al. 2013), our
339 findings show that MitoSOX flashes in flower tissues reflect the nature of the flashes. An
340 increase in the frequency of flashes in the pistil indicates that superoxide flashes together with
341 mitochondrial ROS might be more involved in mitochondrial viability and physiological
342 metabolism in flower pistils. Besides, superoxide flashes were strongly inhibited when electron
343 transport was dysfunction (Wang et al. 2008). Superoxide flashes were markedly decreased by
344 uncoupler of mitochondrial electron transport chain (Zhang et al. 2013). Also, the decrease of cp-

345 YFP fluorescence caused by the addition of ADP and uncoupler FCCP was observed in
346 mitochondria of Arabidopsis, which suggested the superoxide signal appeared to correlate with
347 the magnitude of proton motive force (Schwarzlander et al. 2011). The decreasing of superoxide
348 signal and flashes frequency in our study suggest that a strongly electrical transmembrane
349 gradient is necessary for the production of superoxide flashes.

350 Spontaneous burst superoxide flashes are always consequential to the depolarization of
351 mitochondrial $\Delta\Psi_m$ (Feng et al. 2017). A cp-YFP flash is always accompanied by depolarization
352 of the $\Delta\Psi_m$ (Li et al. 2012). The global rise in mitochondrial basal ROS can trigger the
353 depolarization of $\Delta\Psi_m$ (Zorov et al. 2014) with further stimulation of ROS-induced ROS release
354 resulting in an amplified ROS signal in response to oxidative challenge (Kuznetsov et al. 2017).
355 Reversible variation of $\Delta\Psi_m$ is associated with the release of ROS under different physiological
356 conditions (Kuznetsov et al. 2017). The simultaneous change in the frequency of superoxide
357 flashes and depolarization of the mitochondrial membrane potential in our study suggest that
358 superoxide flashes are always accompanied by fluctuations in the $\Delta\Psi_m$. Although the biogenesis
359 of superoxide flashes is closely related to depolarization of the $\Delta\Psi_m$, the genesis of the flashes is
360 not only related to $\Delta\Psi_m$ fluctuations. The incidence of $\Delta\Psi_m$ fluctuations is higher than that of
361 superoxide flashes, because the cation and anion channels potentially contribute to fluctuation in
362 the $\Delta\Psi_m$ (Wang et al. 2012). Thus, the higher rate of depolarization of $\Delta\Psi_m$ in our study
363 suggests more ion exchange in mitochondria than the incidence of flashes.

364

365

366 **Conclusions**

367 In conclusion, our study presents an efficient method to isolate functional mitochondria to
368 study superoxide flashes. Superoxide flashes visualized by MitoSOX reflect the nature of the
369 flash. Moreover, the simultaneous increase in MitoSOX flashes and depolarization of $\Delta\Psi_m$ in
370 mitochondria isolated from pistils demonstrate that mitochondria are involved in energy

371 metabolism and physiological activities.

372

373

374

375

376

377

378

379

380

381

382 **References**

- 383 Ahanger MA, Tomar NS, Tittal M, Argal S, Agarwal RM (2017) Plant growth under water/salt stress: ROS
384 production; antioxidants and significance of added potassium under such conditions. *Physiol Mol Biol Pla*
385 23:731-744
- 386 Ahmed Z, Fu YB (2015) An improved method with a wider applicability to isolate plant mitochondria for mtDNA
387 extraction. *Plant methods* 11:56
- 388 Cao YX, Zhang X, Shang W, Xu JJ, Wang XH, Hu XQ, Ao YF, Cheng HP (2013) Proinflammatory cytokines
389 stimulate mitochondrial superoxide flashes in articular chondrocytes in vitro and in situ. *PLoS One*
390 8:e66444
- 391 Chakrabarty D, Chatterjee J, Datta SK (2007) Oxidative stress and antioxidant activity as the basis of senescence in
392 chrysanthemum florets. *Plant Growth Regul* 53:107-115
- 393 Day DA, Neuburger M., Douce R (1985) Biochemical characterization of chlorophyll-free mitochondria from pea
394 leaves. *Aust J Plant Physiol* 12:219-228
- 395 Dickinson BC, Chang CJ (2011) Chemistry and biology of reactive oxygen species in signaling or stress responses.
396 *Nat Chem Biol* 7:504-511
- 397 Fang HQ, Chen M, Ding Y, Shang W, Xu JJ, Zhang X, Zhang WR, Li KT, Xiao Y, Gao F, Shang SJ, Li JC, Tian
398 XL, Wang SQ, Zhou JS, Weisleder N, Ma JJ, Ouyang KF, Chen J, Wang XH, Zheng M, Wang W, Zhang
399 XQ, Cheng HP (2011) Imaging superoxide flash and metabolism-coupled mitochondrial permeability
400 transition in living animals. *Cell Res* 21:1295-1304
- 401 Feng G, Liu B, Hou T, Wang X, Cheng H (2017) Mitochondrial flashes: elemental signaling events in eukaryotic
402 cells. *Handb Exp Pharmacol* 240:403-422
- 403 Grabelnych OI, Borovik OA, Tauson EL, Pobezhimova TP, Katyshev AI, Pavlovskaya NS, Koroleva NA,
404 Lyubushkina IV, Bashmakov VY, Popov VN, Borovskii GB, Voinikov VK (2014) Mitochondrial energy-
405 dissipating systems (alternative oxidase, uncoupling proteins, and external NADH dehydrogenase) are
406 involved in development of frost-resistance of winter wheat seedlings. *Biochemistry-Moscow+* 79:506-519
- 407 Hatefi Y (1985) The mitochondrial electron transport and oxidative phosphorylation system. *Annu Rev of Biochem*
408 54:1015-1069
- 409 Hou TT, Zhang X, Xu JJ, Jian CS, Huang ZL, Ye T, Hu KP, Zheng M, Gao F, Wang XH, Cheng HP (2013)
410 Synergistic triggering of superoxide flashes by mitochondrial Ca²⁺ uniport and basal reactive oxygen
411 species elevation. *J Biol Chem* 288:4602-4612
- 412 Jastroch M (2017) Uncoupling protein 1 controls reactive oxygen species in brown adipose tissue. *Proc Natl Acad*
413 *Sci U S A* 114:7744-7746
- 414 Keech O, Dizengremel P, Gardestrom P (2005) Preparation of leaf mitochondria from *Arabidopsis thaliana*. *Physiol*
415 *Plantarum* 124:403-409
- 416 Keunen E, Schellingen K, Van Der Straeten D, Remans T, Colpaert J, Vangronsveld J, Cuypers A (2015)
417 Alternative oxidase1a modulates the oxidative challenge during moderate Cd exposure in *Arabidopsis*
418 *thaliana* leaves. *J Exp Bot* 66:2967-2977
- 419 Kim HY, Botelho SC, Park KJ, Kim H (2015) Use of carbonate extraction in analyzing moderately hydrophobic
420 transmembrane proteins in the mitochondrial inner membrane. *Protein Sci* 24:2063-2069
- 421 Kuznetsov AV, Javadov S, Saks V, Margreiter R, Grimm M (2017) Synchronism in mitochondrial ROS flashes,

- 422 membrane depolarization and calcium sparks in human carcinoma cells. *Biochimica et biophysica acta*
423 1858:418-431
- 424 Li K, Zhang W, Fang H, Xie W, Liu J, Zheng M, Wang X, Wang W, Tan W, Cheng H (2012) Superoxide flashes
425 reveal novel properties of mitochondrial reactive oxygen species excitability in cardiomyocytes. *Biophys J*
426 102:1011-1021
- 427 Luo SX, Chaw SM, Zhang DX, Renner SS (2010) Flower heating following anthesis and the evolution of gall midge
428 pollination in Schisandraceae. *Am J Bot* 97:1220-1228
- 429 Lyu W, Selinski J, Li L, Day DA, Murcha MW, Whelan J, Wang Y (2018) Isolation and respiratory measurements
430 of mitochondria from *Arabidopsis thaliana*. *J Vis Exp* 131:e56627
- 431 Ma Q, Fang HQ, Shang W, Liu L, Xu ZS, Ye T, Wang XH, Zheng M, Chen Q, Cheng HP (2011) Superoxide
432 flashes early mitochondrial signals for oxidative stress-induced apoptosis. *J Biol Chem* 286:27573-27581
- 433 Maksimov N, Evmenyeva A, Breygina M, Yermakov I (2018) The role of reactive oxygen species in pollen
434 germination in *Picea pungens* (blue spruce). *Plant reproduction*
- 435 Miller RE, Grant NM, Giles L, Ribas-Carbo M, Berry JA, Watling JR, Robinson SA (2011) In the heat of the night -
436 alternative pathway respiration drives thermogenesis in *Philodendron bipinnatifidum*. *New Phytol*
437 189:1013-1026
- 438 NavaneethaKrishnan S, Rosales JL, Lee KY (2018) Loss of Cdk5 in breast cancer cells promotes ROS-mediated cell
439 death through dysregulation of the mitochondrial permeability transition pore. *Oncogene* 37:1788-1804
- 440 Paital B, Chainy GB (2014) Effects of temperature on complexes I and II mediated respiration, ROS generation and
441 oxidative stress status in isolated gill mitochondria of the mud crab *Scylla serrata*. *J Therm Biol* 41:104-
442 111
- 443 Pouvreau S (2010) Superoxide flashes in mouse skeletal muscle are produced by discrete arrays of active
444 mitochondria operating coherently. *PloS One* 5:4439-4451
- 445 Rhoads DM, Umbach AL, Subbaiah CC, Siedow JN (2006) Mitochondrial reactive oxygen species. Contribution to
446 oxidative stress and interorganellar signaling. *Plant Physiol* 141:357-366
- 447 Rogers H, Munne-Bosch S (2016) Production and scavenging of reactive oxygen species and redox signaling during
448 leaf and flower senescence: similar but different. *Plant Physiol* 171:1560-1568
- 449 Rogers HJ (2012) Is there an important role for reactive oxygen species and redox regulation during floral
450 senescence? *Plant Cell Environ* 35:217-233
- 451 Schwarzlander M, Logan DC, Fricker MD, Sweetlove LJ (2011) The circularly permuted yellow fluorescent protein
452 cpYFP that has been used as a superoxide probe is highly responsive to pH but not superoxide in
453 mitochondria: implications for the existence of superoxide 'flashes'. *Biochem J* 437:381-387
- 454 Shen EZ, Song CQ, Lin Y, Zhang WH, Su PF, Liu WY, Zhang P, Xu JJ, Lin N, Zhan C, Wang XH, Shyr Y, Cheng
455 HP, Dong MQ (2014) Mitoflash frequency in early adulthood predicts lifespan in *Caenorhabditis elegans*.
456 *Nature* 508:128-132
- 457 Sundaresan M, Yu ZX, Ferrans VJ, Irani K, Finkel T (1995) Requirement for generation of H₂O₂ for platelet-derived
458 growth factor signal transduction. *Science* 270:296-299
- 459 Sweetlove LJ, Taylor NL, Leaver CJ (2007) Isolation of intact, functional mitochondria from the model plant
460 *Arabidopsis thaliana*. *Methods Mol Biol* 372:125-136
- 461 Thien LB, Bernhardt P, Devall MS, Chen ZD, Luo YB, Fan JH, Yuan LC, Williams JH (2009) Pollination biology
462 of basal angiosperms (Anita Grade). *Am J Bot* 96:166-182

- 463 Wang JQ, Chen Q, Wang XH, Wang QC, Wang Y, Cheng HP, Guo CX, Sun QM, Chen Q, Tang TS (2013)
464 Dysregulation of mitochondrial calcium signaling and superoxide flashes cause mitochondrial genomic
465 DNA damage in Huntington Disease. *J Biol Chem* 288:3070-3084
- 466 Wang W, Fang H, Groom L, Cheng A, Zhang W, Liu J, Wang X, Li K, Han P, Zheng M, Yin J, Wang W, Mattson
467 MP, Kao JP, Lakatta EG, Sheu SS, Ouyang K, Chen J, Dirksen RT, Cheng H (2008) Superoxide flashes in
468 single mitochondria. *Cell* 134:279-290
- 469 Wang W, Gong GH, Wang XH, Wei-LaPierre L, Cheng HP, Dirksen R, Sheu SS (2016a) Mitochondrial flash:
470 integrative reactive oxygen species and pH signals in cell and organelle biology. *Antioxid Redox Sign*
471 25:534-549
- 472 Wang X, Jian C, Zhang X, Huang Z, Xu J, Hou T, Shang W, Ding Y, Zhang W, Ouyang M, Wang Y, Yang Z,
473 Zheng M, Cheng H (2012) Superoxide flashes: elemental events of mitochondrial ROS signaling in the
474 heart. *J Mol Cell Cardiol* 52:940-948
- 475 Wang X, Zhang X, Huang Z, Wu D, Liu B, Zhang R, Yin R, Hou T, Jian C, Xu J, Zhao Y, Wang Y, Gao F, Cheng
476 H (2016b) Protons trigger mitochondrial flashes. *Biophys J* 111:386-394
- 477 Wei L, Dirksen RT (2012) Perspectives on: SGP symposium on mitochondrial physiology and medicine:
478 mitochondrial superoxide flashes: from discovery to new controversies. *J Gen Physiol* 139:425-434
- 479 Wei L, Salahura G, Boncompagni S, Kasischke KA, Protasi F, Sheu SS, Dirksen RT (2011) Mitochondrial
480 superoxide flashes: metabolic biomarkers of skeletal muscle activity and disease. *Faseb J* 25:3068-3078
- 481 Yang JL, Mukda S, Chen SD (2018) Diverse roles of mitochondria in ischemic stroke. *Redox biology* 16:263-275
- 482 Yang Y, Karakhanova S, Hartwig W, D'Haese JG, Philippov PP, Werner J, Bazhin AV (2016) Mitochondria and
483 mitochondrial ROS in cancer: novel targets for anticancer therapy. *J Cell Physiol* 231:2570-2581
- 484 Zandalinas SI, Mittler R (2018) ROS-induced ROS release in plant and animal cells. *Free Radical Bio Med* 122:21-
485 27
- 486 Zhang X, Huang Z, Hou T, Xu J, Wang Y, Shang W, Ye T, Cheng H, Gao F, Wang X (2013) Superoxide constitutes
487 a major signal of mitochondrial superoxide flash. *Life sciences* 93:178-186
- 488 Zorov DB, Juhaszova M, Sollott SJ (2014) Mitochondrial reactive oxygen species (Ros) and Ros-Induced Ros
489 Release. *Physiol Rev* 94:909-950

Figure 1

Sampling and detection of isolated mitochondria.

Sampling of *Magnolia denudata* (A) and *Nelumbo nucifera* (F). Detection of auto-fluorescence of intact chloroplasts in *M. denudata* (B) and *N. nucifera* (G). Viability of isolated mitochondria in petal (C) and style (D) of *M. denudata*, petal (H) and receptacle (I) of *N. nucifera* using our efficiency method A (crude isolated mitochondria). Viability of mitochondria isolated from style in *M. denudata* (E) and from receptacle in *N. nucifera* (J) using method B (density gradient-purified mitochondria). Pe: petal, Gy: gynoecium, Rec: receptacle. Scale bar: 5 μ m.(All photos were taken by Chulan Zhang).

*Note: Auto Gamma Correction was used for the image. This only affects the reviewing manuscript. See original source image if needed for review.

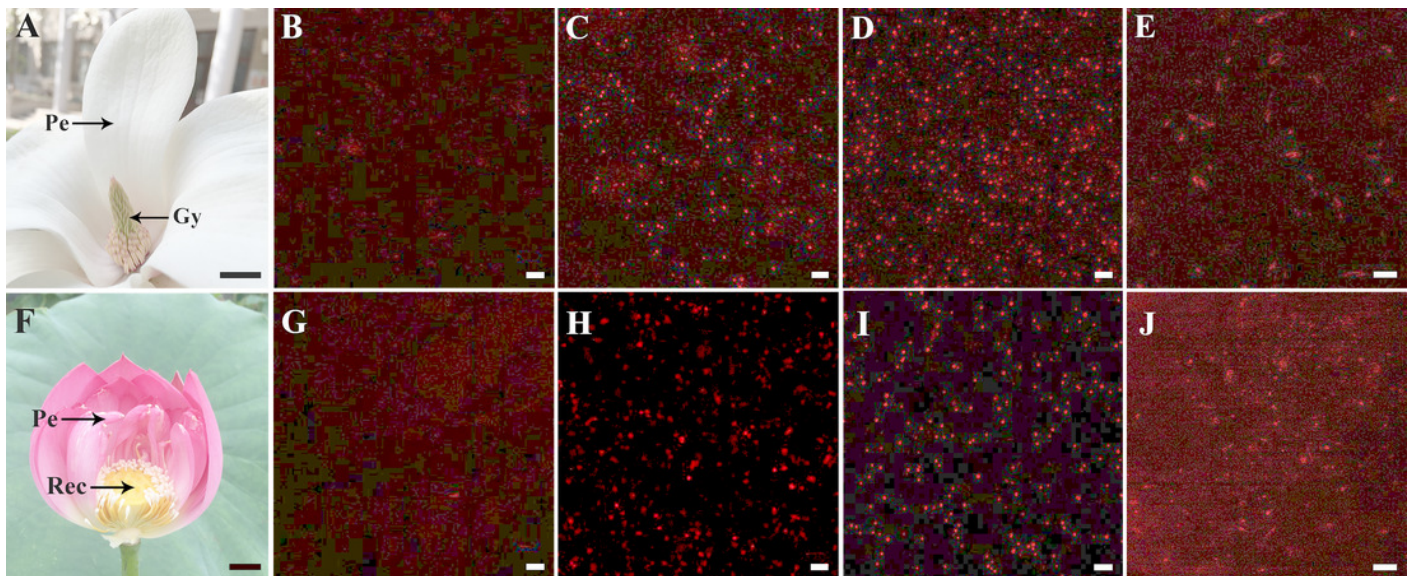


Figure 2

ROS production and colocalization with mitochondria.

ROS production and colocalization with mitochondria isolated from *M. denudata*:

mitochondria isolated from petal (A) and style (E) were visualized by Mito Tracker Green (in green color), mitochondrial ROS in mitochondria isolated from petal (B) and mitochondria isolated from style (F) was visualized by MitoSOX red (in red color), colocalization of ROS and mitochondria in petal (C) and style (G). D. Comparison of ROS fluorescent intensity in petal and style of *M. denudata*. ROS production and colocalization with mitochondria isolated from *N. nucifera*: mitochondria isolated from petal (H) and receptacle (L) were visualized by Mito Tracker Green (in green color), mitochondrial ROS in mitochondria isolated from petal (I) and mitochondria isolated from style (M) was visualized by MitoSOX red (in red color), colocalization of ROS and mitochondria in petal (J) and receptacle (N). K. Comparison of ROS fluorescent intensity in petal and receptacle of *N. nucifera*. Scale bar: 5 μ m.

**Note: Auto Gamma Correction was used for the image. This only affects the reviewing manuscript. See original source image if needed for review.*

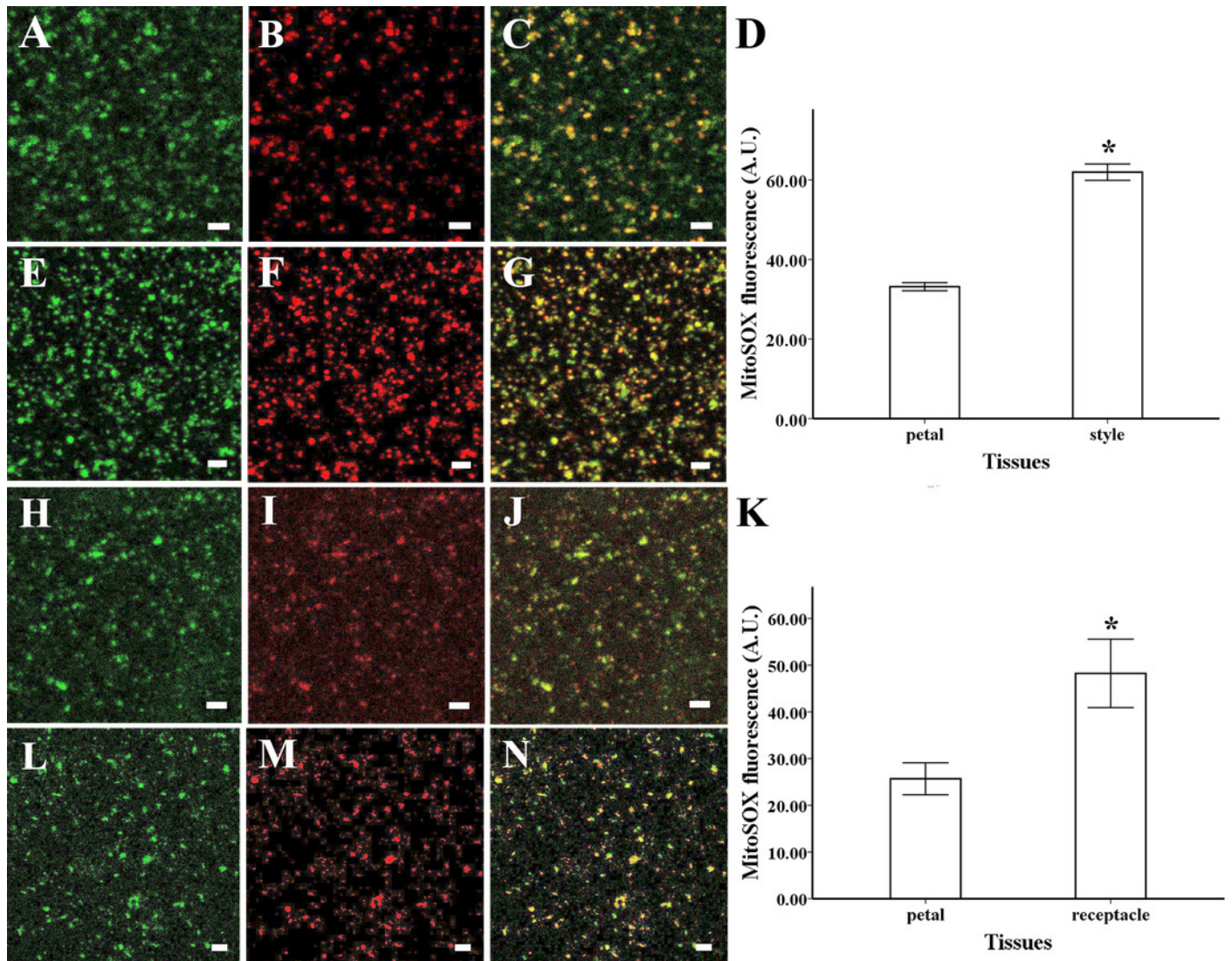


Figure 3

Superoxide flashes visualized by MitoSOX and flashes frequency.

A. Isolated mitochondria labeled with MitoSOX red. B. Time-lapse images (upper) and typical trace (lower panel) of superoxide flashes visualized by MitoSOX red. Different types of traces of superoxide flashes (C) low variation slope traces, (D) high variation slope traces, (E) multi-event traces. F. Comparison of superoxide flashes frequency in mitochondria isolated from petal and style of *M. denudata*. G. Comparison of superoxide flashes frequency in mitochondria isolated from petal and receptacle of *N. nucifera*. Scale bar: 5 μ m.

**Note: Auto Gamma Correction was used for the image. This only affects the reviewing manuscript. See original source image if needed for review.*

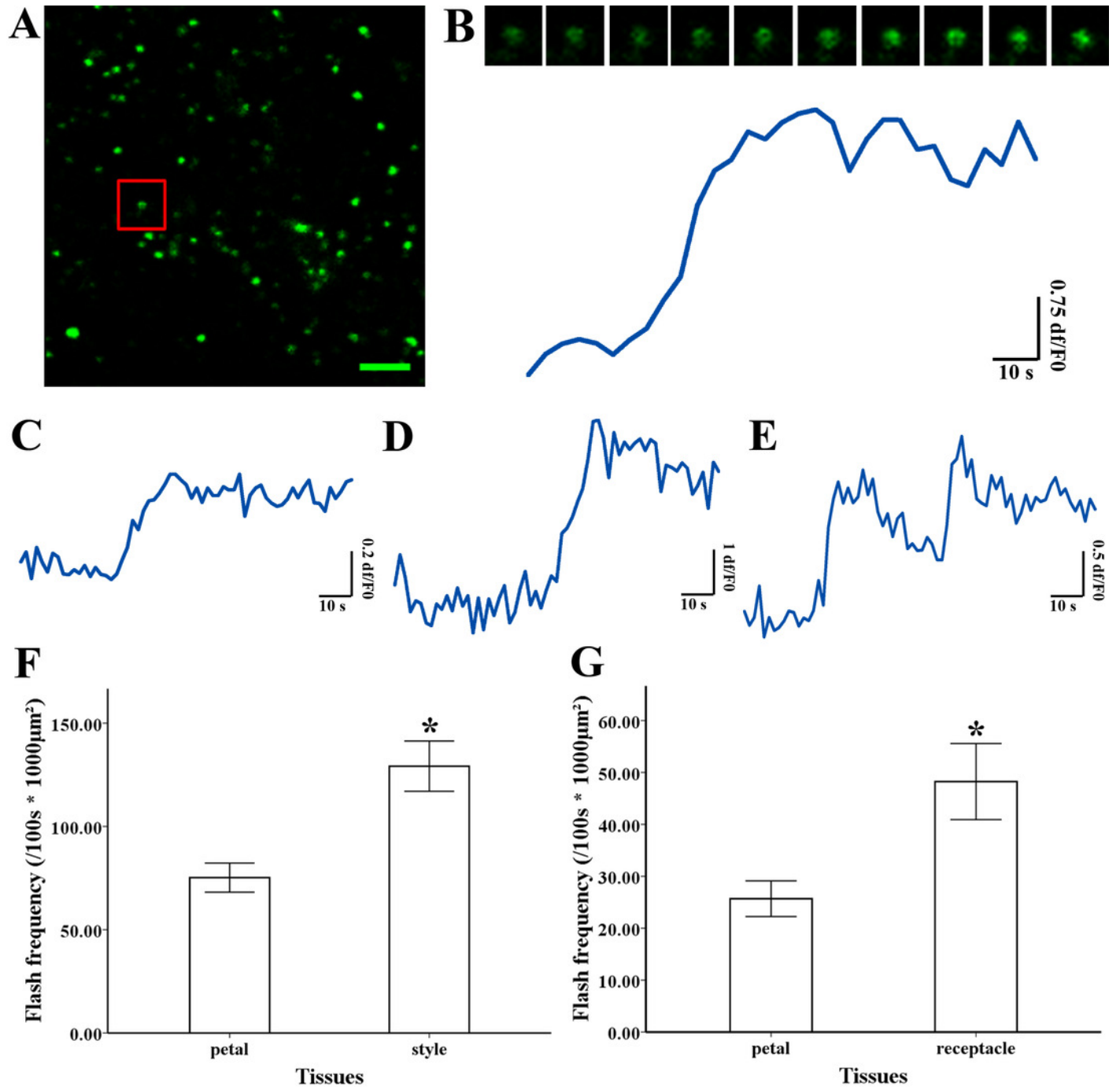


Figure 4

ROS production and superoxide flashes in different respiratory substrate.

Isolated mitochondria from style of *M. denudata* labeled with MitoSOX red (A) 5 mM succinate, (B) 5 mM succinate and 250 μ M ADP, (C) 5 mM succinate and 5 μ M FCCP.

Comparison of ROS production and superoxide flashes frequency in mitochondria isolated from style of *M. denudata* in different respiratory substrate: (D). Comparison of mitochondrial ROS fluorescent intensity in different respiratory substrate. (E). Comparison of mitochondrial superoxide flashes frequency in different respiratory substrate. succ: succinate. Scale bar: 5 μ m.

*Note: Auto Gamma Correction was used for the image. This only affects the reviewing manuscript. See original source image if needed for review.

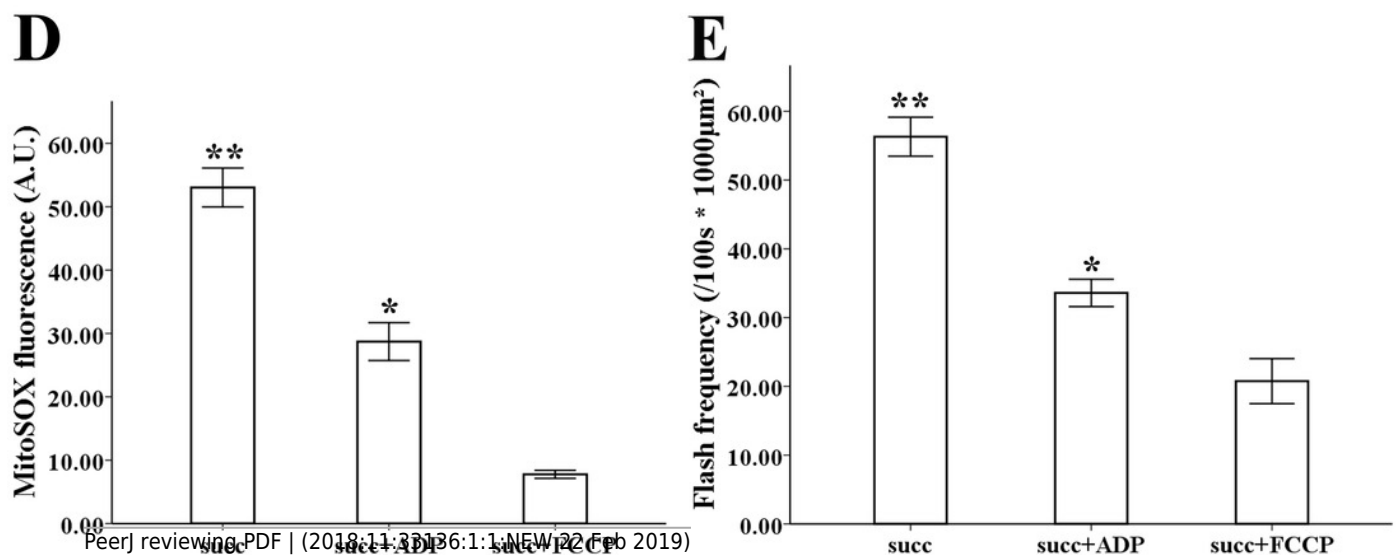
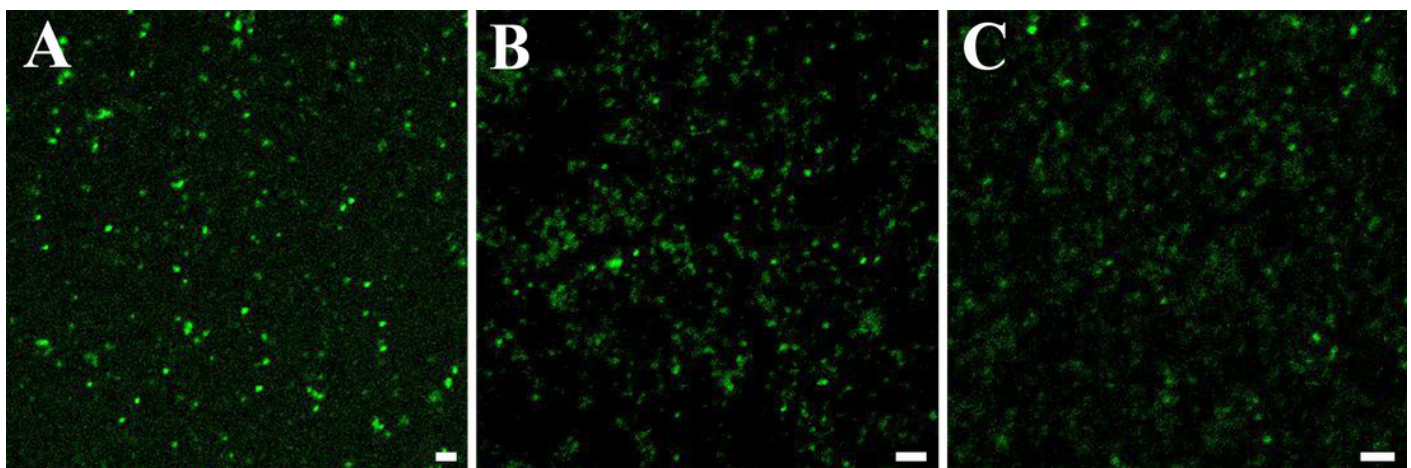


Figure 5

Depolarization of mitochondria membrane potential ($\Delta\Psi_m$) and frequency.

A. Isolated mitochondria labeled by TMRM. B. Time-lapse images (upper) and typical trace (lower panel) of depolarization of $\Delta\Psi_m$ labeled by TMRM. Different types of trace of TMRM (C) instantaneous loss and recovery of $\Delta\Psi_m$, (D) instantaneous loss with the short period of stability before recovery of $\Delta\Psi_m$, (E) multi-event traces. Comparison of depolarization of $\Delta\Psi_m$ frequency in mitochondria isolated from petal and style of *N. nucifera* (F). Comparison of depolarization of $\Delta\Psi_m$ frequency in mitochondria isolated from petal and receptacle of *M. denudata* (G). Scale bar: 5 μ m.

**Note: Auto Gamma Correction was used for the image. This only affects the reviewing manuscript. See original source image if needed for review.*

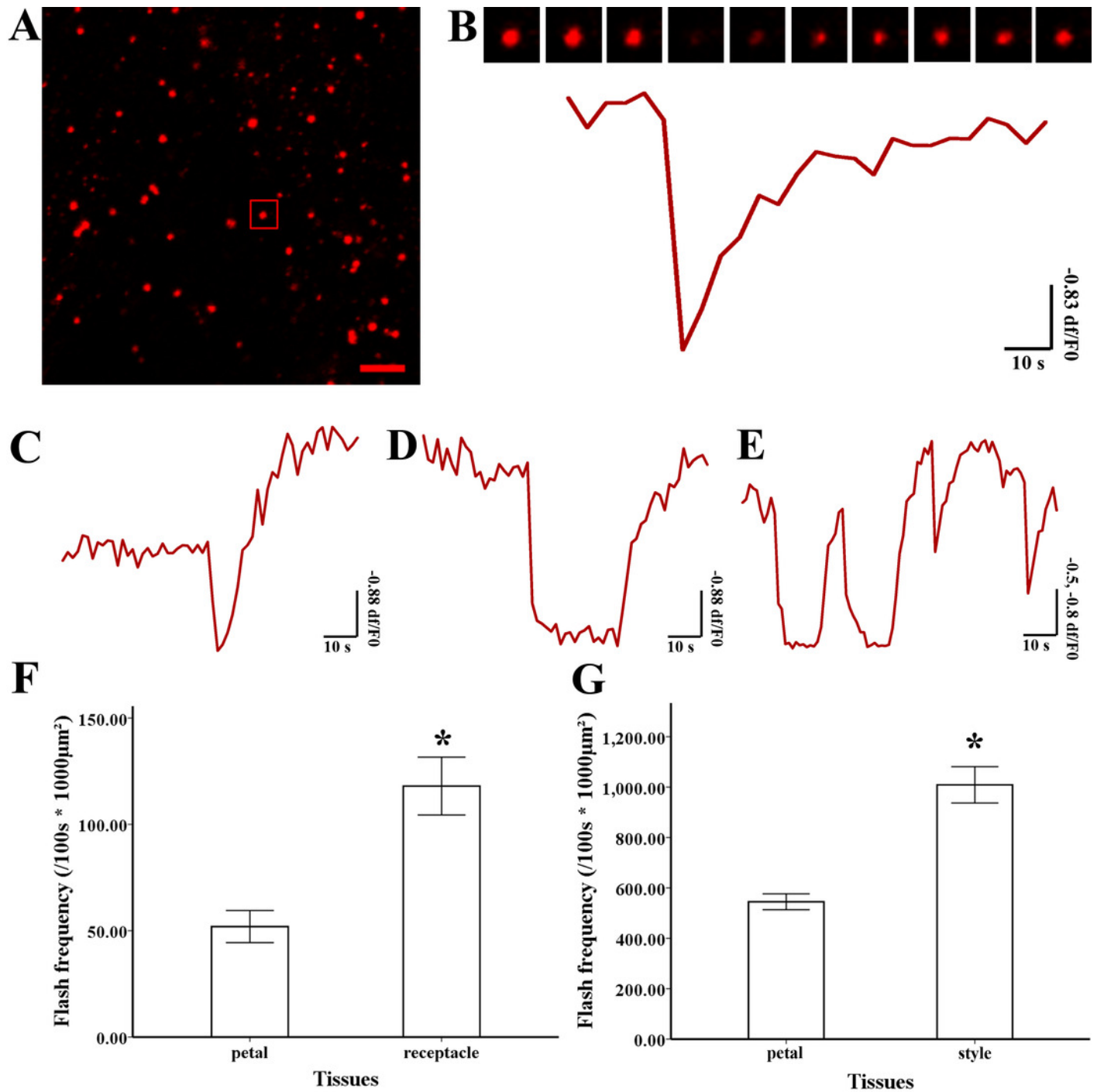


Table 1 (on next page)

Respiratory function of isolated mitochondria.

Respiratory function of isolated mitochondria isolated from pistils and petal tissues of *Magnolia denudata* and *Nelumbo nucifera* with our efficiency method A (crude isolated mitochondria) and respiration function of isolated mitochondria from style of *Magnolia denudata* with previous method B (density gradient-purified mitochondria). Values are mean \pm S.D., n=6.

1

2

Table 1

Respiratory function of isolated mitochondria with our method A and previous method B

Groups	State 3 nmol O \cdot min $^{-1}\cdot$ mg $^{-1}$	State 4 nmol O \cdot min $^{-1}\cdot$ mg $^{-1}$	RCR
Stigma (<i>M. denudata</i>)	269.68 \pm 28.49	60.08 \pm 6.13	4.49 \pm 0.20 ^a
Petal (<i>M. denudata</i>)	276.06 \pm 31.50	64.46 \pm 7.88	4.29 \pm 0.16 ^{ab}
Receptacle (<i>N. nucifera</i>)	257.73 \pm 34.91	60.00 \pm 8.59	4.30 \pm 0.21 ^{ab}
Petal (<i>N. nucifera</i>)	259.14 \pm 33.82	61.99 \pm 8.68	4.19 \pm 0.25 ^b
Method B	243.90 \pm 35.01	61.89 \pm 8.39	3.94 \pm 0.18 ^c

Values are mean \pm S.D., n=6.

3

4